Real-time monitoring of superoxide anion radical generation in response to wounding: *in vivo* electrochemical study

Ankush Prasad [Corresp., 1, 2] , **Aditya Kumar** [3] , **Ryo Matsuoka** [4] , **Akemi Takahashi** [5] , **Ryo Fujii** [5] , **Yamato Sugiura** [5] , **Hiroyuki Kikuchi** [5] , **Shigeo Aoyagi** [4] , **Tatsuo Aikawa** [6] , **Takeshi Kondo** [6] , **Makoto Yuasa** [6] , **Pavel Pospíšil** [3] , **Shigenobu Kasai** [2, 5]

[1] Department of Biophysics, Centre of the Region Haná for Biotechnological and Agricultural Research, Faculty of Science, Palacký University, Olomouc, Czech Republic

[2] Biomedical Engineering Research Center, Tohoku Institute of Technology, Sendai, Japan

[3] Department of Biophysics, Centre of the Region Haná for Biotechnological and Agricultural Research, Olomouc, Czech Republic

[4] Hokuto Denko Corporation, Tokyo, Japan

[5] Graduate Department of Environmental Information Engineering, Tohoku Institute of Technology, Sendai, Japan

[6] Department of Pure and Applied Chemistry, Tokyo University of Science, Noda, Chiba, Japan

Corresponding Author: Ankush Prasad
Email address: prasad.ankush@gmail.com

Background: The growth and development of plants is deleteriously affected by various biotic and abiotic stress factors. Wounding in plants is caused by exposure to environmental stress, mechanical stress, and via herbivory. Typically, oxidative burst in response to wounding is associated with the formation of reactive oxygen species, such as the superoxide anion radical ($O_2^{\bullet-}$), hydrogen peroxide (H_2O_2) and singlet oxygen; however, few experimental studies have provided direct evidence of their detection in plants. Detection of $O_2^{\bullet-}$ formation in plant tissues have been performed by using various techniques including electron paramagnetic resonance spin-trap spectroscopy, epinephrine-adrenochrome acceptor methods, staining with dyes such as tetrazolium dye and nitro blue tetrazolium (NBT), however, kinetic measurements have not been performed. In the current study, we provide evidence of $O_2^{\bullet-}$ generation and it kinetics in the leaves of spinach (*Spinacia oleracea*) subjected to wounding.

Methods: Real-time monitoring of $O_2^{\bullet-}$ generation was performed using catalytic amperometry. Changes in oxidation current for $O_2^{\bullet-}$ was monitored using polymeric iron-porphyrin-based modified carbon electrodes (φ=1 mm) as working electrode with Ag/AgCl as the reference electrode.

Result: The results obtained show continuous generation of $O_2^{\bullet-}$ for minutes after wounding, followed by a decline. The exogenous addition of superoxide dismutase, which is known to dismutate $O_2^{\bullet-}$ to H_2O_2, significantly suppressed the oxidation current.

Conclusion: Catalytic amperometric measurements were performed using polymeric iron-porphyrin based modified carbon electrode. It is claimed to be a useful tool and a direct method for real-time monitoring and precise detection of $O_2^{\bullet-}$ in biological samples. It is claimed to bear a potential for its wide application in plant research for specific and sensitive detection of $O_2^{\bullet-}$.

1   **Real-time monitoring of superoxide anion radical generation in**

2   **response to wounding: electrochemical study**

3   Ankush Prasad[1,2*], Aditya Kumar[1], Ryo Matsuoka[3], Akemi Takahashi[4], Ryo Fujii[4], Yamato

4   Sugiura[4], Hiroyuki Kikuchi[4], Shigeo Aoyagi[3], Tatsuo Aikawa[5], Takeshi Kondo[5], Makoto Yuasa[5],

5   Pavel Pospíšil[1], Shigenobu Kasai[#2,4]

8   [1]Department of Biophysics, Centre of the Region Haná for Biotechnological and Agricultural

9   Research, Faculty of Science, Palacký University, Olomouc, Czech Republic

10   [2]Biomedical Engineering Research Center, Tohoku Institute of Technology, Sendai, Japan.

11   [3]Hokuto Denko Corporation, Tokyo, Japan

12   [4]Graduate Department of Environmental Information Engineering, Tohoku Institute of

13   Technology, Sendai, Japan.

14   [5]Department of Pure and Applied Chemistry, Tokyo University of Science,

15   Noda, Chiba, Japan

19   *Corresponding author: Ankush Prasad, Department of Biophysics, Centre of the Region Haná

20   for Biotechnological and Agricultural Research, Faculty of Science, Palacký University,

21   Šlechtitelů 27, 783 71 Olomouc, Czech Republic.

22   Tel. +420-58563-4752; fax: +420 585225737; E-mail address: ankush.prasad@upol.cz

23   [#]Co-corresponding author: kasai@tohtech.ac.jp

25   **ABSTRACT**

26 **Background:**

27 The growth and development of plants is deleteriously affected by various biotic and abiotic

28 stress factors. Wounding in plants is caused by exposure to environmental stress, mechanical

29 stress, and via herbivory. Typically, oxidative burst in response to wounding is associated with

30 the formation of reactive oxygen species, such as the superoxide anion radical ($O_2^{\bullet-}$), hydrogen

31 peroxide (H_2O_2) and singlet oxygen; however, few experimental studies have provided direct

32 evidence of their detection in plants. Detection of $O_2^{\bullet-}$ formation in plant tissues have been

33 performed using various techniques including electron paramagnetic resonance spin-trap

34 spectroscopy, epinephrine-adrenochrome acceptor methods, staining with dyes such as

35 tetrazolium dye and nitro blue tetrazolium (NBT), however, kinetic measurements have not been

36 performed. In the current study, we provide evidence of $O_2^{\bullet-}$ generation and its kinetics in the

37 leaves of spinach (*Spinacia oleracea*) subjected to wounding.

38 **Methods:**

39 Real-time monitoring of $O_2^{\bullet-}$ generation was performed using catalytic amperometry. Changes

40 in oxidation current for $O_2^{\bullet-}$ was monitored using polymeric iron-porphyrin-based modified

41 carbon electrodes (φ=1 mm) as working electrode with Ag/AgCl as the reference electrode.

42 **Result:**

43 The results obtained show continuous generation of $O_2^{\bullet-}$ for minutes after wounding, followed

44 by a decline. The exogenous addition of superoxide dismutase, which is known to dismutate $O_2^{\bullet-}$

45 to H_2O_2, significantly suppressed the oxidation current.

46

47 **Conclusion:**

48 Catalytic amperometric measurements were performed using polymeric iron-porphyrin based

49 modified carbon electrode. It is claimed to be a useful tool and a direct method for real-time

50 monitoring and precise detection of $O_2^{\bullet-}$ in biological samples. It is claimed to bear a potential

51 for its wide application in plant research for specific and sensitive detection of $O_2^{\bullet-}$.

52

53

54

55

56

57

58

59

60

61

62

63

64

65

66

67

68

69

70 **INTRODUCTION**

71   The formation of reactive oxygen species (ROS) in plants is an unavoidable consequence

72   of photosynthesis [1-4]. The introduction of molecular oxygen into the environment by

73   photosynthetic organisms during the evolution of aerobic life is associated with the formation of

74   ROS [5]. Plants growing in a fluctuating environment are exposed to various biotic stresses such

75   as bacteria, viruses, fungi, parasites, insects, weeds, etc. and abiotic stresses such as fluctuations

76   in temperature, salinity, water, radiation, toxic chemicals and mechanical stress which are closely

77   linked to higher ROS production. The chloroplasts, mitochondria, and peroxisomes are among

78   the chief organelles involved [6-11]. As a response, ROS, including the superoxide anion radical

79   ($O_2^{\bullet-}$), hydroperoxyl radical ($HO_2^{\bullet-}$), hydrogen peroxide (H_2O_2), hydroxyl radical ($HO^{\bullet}$), singlet

80   oxygen ($^1O_2$), peroxyl radical ($ROO^{\bullet}$), hydroperoxide ($ROOH$) and alkoxyl radical ($RO^{\bullet}$), are

81   produced [12-18].

82   The production of ROS by an oxidative burst is an imperative element of the wound

83   response in algae, plants, and animals [19]. As a response to wounding, plants release

84   oligosaccharide cell wall fragments, which play an important role in the signaling cascade that

85   initiates an intense, localized production of ROS [20-22]. Wounding stimulates the production of

86      $O_2^{\bullet-}$, H_2O_2 and nitric oxide (NO), which can directly attack encroaching pathogens at the site of

87   the wound [23-25]. In *Arabidopsis thaliana* leaves measured under ambient light conditions, $O_2^{\bullet-}$

88   and H_2O_2 mainly originate from photosynthetic electron transport, predominantly at the site of

89   wounding [26]. The role of NADPH oxidase in ROS production, however, was not completely

90   ruled out. Therefore, the generation of $O_2^{\bullet-}$ and H_2O_2 can be attributed to the collective effect of

91   wounding and light stress. $O_2^{\bullet-}$ generation in the root cells of plants in response to wounding has

92   been studied by electron paramagnetic resonance (EPR) spin-trap spectroscopy and epinephrine-

93   adrenochrome acceptor methods [27]. Tiron (4, 5-dihydroxy-1, 3-benzene-disulfonic acid

94   disodium salt) was used, and the tiron semiquinone EPR spectra showed $O_2^{\bullet-}$ generation. The

95   level of $O_2^{\bullet-}$ production in the roots was measured with epinephrine which, in the presence of

96   $O_2^{\bullet-}$, is converted to adrenochrome and can be monitored at 480 nm by a spectrophotometer [28,

97   29]. In addition to spectroscopy, staining with dye, such as tetrazolium dye and nitro blue

98   tetrazolium (NBT), has been used to detect the production of $O_2^{\bullet-}$ *in situ*, with visualization of

99   $O_2^{\bullet-}$ generation as a purple formazan deposit within leaflet tissues [30].

100   Although various methods, such as EPR spin-trapping spectroscopy [31],

101   chemiluminescence [32], the reduction of NBT [37, 38] and the reduction of the redox protein

102   cytochrome c [33-35] have been used to detect and monitor $O_2^{\bullet-}$, each of these methods has

103   inadequate specificity and sensitivity. EPR spin-trapping spectroscopy is one of the most

104   sensitive and specific method for ROS detection; however, kinetic measurements are not

105   possible at the current stage of development. Chemiluminescence, also known as ultra-weak

106   photon emission, has been widely used recently as a non-invasive method to understand the

107   involvement of ROS in oxidative radical reactions [36-38]; however, limitations with respect to

108   the specificity for particular ROS involvement exists [39].

109   Integration of metalloporphyrins into electropolymerized polymer electrodes have been

110   developed rigorously over the last years because these materials are effective electrocatalysts for

111   chemical as well as photochemical applications [40]. Numerous authors have recently tested the

112   potential use of electropolymerized metalloporphyrins as new electrode materials for chemical

113   and biological sensors [41-43]. In our current study, we provide an experimental approach for the

114   detection of $O_2^{\bullet-}$ by polymeric iron-porphyrin-based modified carbon electrode based on the

115   reaction mechanism presented in Fig. 1A (Yuasa & Oyaizu, 2005). Detection of $O_2^{\bullet-}$ by highly

116   sensitive and selective polymeric iron-porphyrin-based modified carbon electrodes was tested in

117 *in vivo* leaf sample subjected to wounding. The current study introduces the use of catalytic

118 amperometric biosensors for the real-time detection of $O_2^{\bullet-}$.

119

120 **MATERIAL AND METHODS**

121

122 ***Spinach leaves***

123 Young spinach (*Spinacia oleracea)* leaves were washed twice with deionized water and

124 were dark adapted for 2 hours. For each measurement, a fresh spinach leaf of the approximately

125 same age was chosen. All experiments were performed at room temperature under dark

126 conditions to avoid interference from light sources.

127

128 ***Material and chemical reagents***

129 The 5-(ethoxycarbonyl)-5-methyl-1-pyrroline N-oxide (EMPO) spin trap and capillary

130 tubes used for EPR measurements were obtained from Alexis Biochemicals (Lausen,

131 Switzerland) and Blaubrand intraMARK (Brand, Germany), respectively. The carbon electrodes

132 (φ=1 mm) were purchased from BAS Inc., ALS Co., Ltd. (Tokyo, Japan). Superoxide dismutase

133 (SOD), xanthine oxidase and xanthine (X/XO) were purchased from Wako Pure Chemicals

134 Industries, Ltd. (Osaka, Japan), Sigma-Aldrich chemie Gmbh (Munich, Germany) or Sigma-

135 Aldrich Japan K.K. (Tokyo, Japan).

136

137 ***Equipment and methods***

138 Simultaneous measurements of the oxidation current of $O_2^{\bullet-}$ were performed using a

139 potentiostat (HA1010mM4S; Hokuto Denko Co., Ltd., Japan). The polymeric iron-porphyrin-

140   based modified carbon electrodes were positioned 1 mm from the site of injury using a motor-

141   driven XYZ-stage (K101-20MS-M, Suruga Seiki Co., Ltd., Japan) (Fig. 1B). The detection of

142    $O_2^{\bullet-}$ in the X/XO system was performed by EPR spin-trapping spectroscopy using 25 mM

143   EMPO in phosphate buffer.

144

145   ***Experimental conditions for real-time monitoring of the oxidation current of $O_2^{\bullet-}$***

146   The electrochemical detection of $O_2^{\bullet-}$ was measured using the X/XO system based on the

147   method described in our recent study [44] (Fig. 2). The subsequent oxidation current for $O_2^{\bullet-}$ was

148   monitored using polymeric iron-porphyrin-based modified carbon electrodes (φ=1 mm) with

149   Ag/AgCl as the reference electrode.

150   Spinach leaves were fixed on a petri-dish with a diameter of 60 mm using double-sided

151   adhesive tape. 10 mM Phosphate buffer saline (pH 7.2) (PBS) was gradually added to maintain a

152   sufficient volume to submerge the whole spinach leaf in PBS. During the measurement, injury

153   was performed using glass capillary with an inner diameter of about 1.2mm and wall thickness of

154   200μm. (Fig. 1B and DataS1). Mechanical injury and mechanical wounding were performed

155   close to the site of the electrode. The oxidation current was measured at +0.5 V vs. Ag/AgCl at

156   room temperature.

157

158   ***Superoxide anion radical detection using polymeric iron-porphyrin-based modified carbon***

159   ***electrodes***

160   The detection of $O_2^{\bullet-}$ was based on catalytic amperometry using a counter electrode and

161   working electrode. The counter electrode was a platinum wire (ϕ0.25$\times$ 40 mm), and the working

162   electrode (φ1 mm) was a polymeric iron-porphyrin-based modified carbon electrode. Ag/AgCl

163   was used as a reference electrode. The polymeric iron-porphyrin-based modified carbon

164   electrode acted as an $O_2^{\bullet-}$ detection sensor. The polymeric iron-porphyrin-based modified carbon

165   electrode was prepared by the electropolymerization of 1-methylimidazole-coordinated

166   mesotetra (3-thienyl) porphyrin ([Fe(im)$_2$(ttp)]Br) (Yuasa & Oyaizu, 2005; Yuasa et al., 2005).

167   Electropolymerization was performed in a two-chamber three-electrode electrochemical cell by

168   potential cycling from 0 to +2.0 V vs. Ag/Ag$^+$ with a potential sweep rate of 50 mV s^{-1}. After

169   rinsing with dichloromethane, the polymeric iron-porphyrin-based modified carbon electrode

170   was obtained (Yuasa & Oyaizu, 2005; Yuasa et al., 2005). For the basic characterization of the

171   polymeric iron-porphyrin-based modified carbon electrode, a differential pulse voltammogram of

172   the electropolymerized [Fe(im)$_2$(ttp)]Br complex was recorded in an aqueous electrolyte solution

173   containing 10 mM PBS (pH 7.2) using a high-performance potentiostat HZ-7000 (Hokuto Denko

174   Co., Ltd., Japan) (supplementary data S2).

175

176

177   **RESULTS**

178   ***Characterization and sensitivity evaluation of an iron-porphyrin-based modified carbon***

179   ***electrode***

180   The characterization of the polymeric iron-porphyrin-based modified carbon electrode

181   was performed using a differential pulse voltammogram (DPV) (supplementary data S2). The

182   polymerized complex was electroactive, with a mean redox potential at -0.25 V for the Fe^{2+}/Fe^{3+}

183   couple.

184

185 ***Generation of $O_2^{\bullet-}$ in the chemical system and sensitivity evaluation of the polymeric iron-***

186 ***porphyrin-based modified carbon electrode***

187 The xanthine/xanthine oxidase system is used for the formation of $O_2^{\bullet-}$ by the reduction

188 of molecular oxygen [45-47]. To confirm the formation of $O_2^{\bullet-}$ in the chemical system used in

189 the later experimental procedures, we measured the EMPO-OOH adduct EPR signal

190 (supplementary data S3: A). The intensity of the EMPO-OOH adduct EPR signal in the control

191 (xanthine) and chemical system (X/XO) was also measured (supplementary data S3: B). In the

192 absence of xanthine oxidase, no EMPO-OOH adduct EPR signal was observed, whereas in the

193 presence of XO, an EMPO-OOH adduct EPR signal was observed (supplementary data S3).

194 To determine the sensitivity of the polymeric iron-porphyrin-based modified carbon

195 electrode, the response of the exogenous addition of a standard known concentration of $O_2^{\bullet-}$

196 generated *in situ* was measured using X/XO system. A linear increase in oxidation current was

197 observed with an increase in $O_2^{\bullet-}$ concentration. The calibration curve (Δi vs $O_2^{\bullet-}$) was found to

198 be linear in the concentration range of 0.4 to 1.3μM (Fig. 2). This indicates that the sensitivity of

199 the electrochemical sensor is in the range of μM concentration, reflecting changes in the

200 oxidation current in the order of tens of nA (Fig. 2).

201

202 ***Real-time monitoring of $O_2^{\bullet-}$ generation during wounding of spinach leaves***

203 To validate that there is no interference in the measurement caused by the suspension of

204 spinach leaf in PBS, the oxidation current was measured in a non-wounded spinach leaf

205 suspended in PBS as indicated by the arrow, during the real-time measurement (Fig. 3). No

206 fluctuation in the oxidation current of $O_2^{\bullet-}$ was observed in the non-wounded spinach leaf

207 suspended in PBS, (Fig. 3), whereas a negligible fluctuation was observed with the exogenous

208   addition of SOD (data not shown). These results indicate that these chemical species (PBS and

209   SOD) do not interfere with the measurements. The kinetics of the production of $O_2^{\bullet-}$ were also

210   measured in the chemical system containing no spinach leaves and in the presence of SOD (400

211   U ml^{-1}) indicating no significant fluctuation in oxidation current (supplementary data S4).

212   Real-time monitoring of the oxidation current for $O_2^{\bullet-}$ was performed in spinach leaves

213   where mechanical injury was stimulated 1 time using glass tube (Fig. 4A) and mechanical

214   wounding was done multiple times (Fig. 4B). The wounding in spinach leaves was done 1 time

215   (4A) and multiple times (between 8-10 tims) using a glass capillary with an inner diameter of

216   about 1.2mm and wall thickness of 200μm). The results indicate that the $O_2^{\bullet-}$ production

217   increased considerably with the dose of mechanical injury (Fig. 4). Furthermore, to visualize the

218   extent of damage to leaf during mechanical injury induced by glass capillary, photograph of

219   leaves showing the physiological state have been presented along with kinetics on real-time

220   monitoring of the oxidation current of $O_2^{\bullet-}$ under experimental condition mentioned in dataset

221   presented (Data S1). To determine the concentration of $O_2^{\bullet-}$ generated in mechanically injured

222   spinach leaves, the calibration curve was established for various concentrations obtained using

223   standard X/XO system (Fig. 2). A maximum oxidation current ($\triangle$i) of 1.5 nA (at time span, 60

224   sec) and 7.5 nA (at time span, 300 sec) was observed in mechanically injury made at a minimal

225   dose (Fig. 4A) and at multiple sites (Fig. 4B). Based on the data obtained and the maximum

226   oxidation current recorded, the $O_2^{\bullet-}$ was calculated and expected production was found to be

227   about 40 nM (4A) and 200 nM (4B) (Table 1).

228   In addition, $O_2^{\bullet-}$ generation was also measured in spinach leaves under the effect of

229   wounding at room temperature in presence of exogenous addition of SOD (Fig. 5). In the

230   absence of wounding, as observed during the first minute of real-time monitoring, no

231   considerable change in the oxidation currents of $O_2^{\bullet-}$ was observed. However, wounding

232   instantaneously resulted in a fast increase in the oxidation current for $O_2^{\bullet-}$ of approximately 10

233   nA, followed by a gradual decrease, which continued for more than 10 min. To confirm the

234   production of $O_2^{\bullet-}$, the effect of SOD, which leads to the dismutation of $O_2^{\bullet-}$ to H_2O_2, on the

235   oxidation current in a wounded spinach leaf was analyzed. The addition of 400 U ml^{-1} SOD

236   suppressed the oxidation current for $O_2^{\bullet-}$ from 3.5 nA to 2 nA (Fig. 5). However, complete

237   suppression of the oxidation current was not observed. The oxidation current, which persisted at

238   approximately 1 nA for a few minutes, can be attributed to rapid $O_2^{\bullet-}$ diffusion to the electrode

239   before its conversion to H_2O_2 or to the limited SOD activity at a fixed concentration. The effect

240   of SOD (400 U ml^{-1}) added exogenously was also measured at the point of maximum oxidation

241   current where a comparatively higher suppression was recorded (Fig. 6).

242

243   **DISCUSSION**

244   In addition to plants, ROS detections have been performed in model system including

245   animals. During recent past, Zuo and coworkers presented results on intracellular ROS formation

246   in single isolated frog myofibers during low P_{O2} conditions using dihydrofluorescein (Hfluor), a

247   fluorescein analog of DCFH [48,49]. Cyt c assay was also used to measure $O_2^{\bullet-}$ in contracting

248   skeletal muscle in pulmonary TNF-α overexpression mice [50, 51]. Several mechanisms for the

249   generation of ROS involving $O_2^{\bullet-}$ have been suggested. It has been proposed previously that an

250   NADPH oxidase-like enzyme in the plant plasma membrane is involved in the production of $O_2^{\bullet-}$,

251   which is then converted to the more stable H_2O_2 during the oxidative burst in response to

252   pathogen attack of plant cells [52, 53]. In skeletal muscle, the major source of ROS especially

253   extracellular $O_2^{\bullet-}$ formation is via the arachidonic acid metabolism through lipoxygenase (LOX)

254 activity [51]. However, in contrast to the view that wound-induced ROS are primarily produced

255 extracellularly by NADPH oxidase enzymes [54, 55], it has been recently indicated that wound-

256 induced $O_2^{\bullet-}$ and H_2O_2 originate from photosynthetic electron transport measured at wounded

257 sites under ambient light conditions [26]. The $O_2^{\bullet-}$ is produced during the electron transport

258 process by the reduction of molecular oxygen in the chloroplasts and mitochondria. The authors

259 proposed that $O_2^{\bullet-}$ and H_2O_2 production is linked to wounding, which is enhanced significantly

260 under light conditions.

261   A recent report on *Pisum sativum* seedlings proposes a mechanism responsible for

262 oxidative burst during wounding. During mechanical wounding, polyunsaturated fatty acids

263 (PUFA), polyamines, LOX and peroxidases (Prx) are released in the extracellular matrix. Under

264 these circumstances, LOX is involved in the oxidation of PUFA or polyamines, which induces

265 diamine oxidases (DAO) to produce H_2O_2, further leading to $O_2^{\bullet-}$ production catalyzed by Prx

266 [56]. A diverse range of organisms use Prx to produce $O_2^{\bullet-}$, e.g., *Triticum sativum* roots [57],

267 *Castanea sativa* and *Trichilia* seeds [58, 59], liverworts [60], and lichens [61]. Another group of

268 redox enzyme involved in the wound-induced oxidative burst is DAO [62-65], and cooperation

269 between DAO and Prx is considered important in the wound response. In addition to DAO and

270 Prx, LOX not only generates lipid hydroperoxides (LOOH) but can also generate $O_2^{\bullet-}$ via the

271 oxidation of pyridine nucleotides and therefore considerably contributes to oxidative stress in

272 cells [66]. Lipid oxidation by LOX is an important part of the wound-response because oxylipins,

273 the break-down products of lipid peroxides, can act as effective signaling molecules to rapidly

274 induce transcriptional changes during wounding [67, 68]. Plasma membrane-bound Prx can

275 utilize PUFA such as linoleic acid released at the wound site for the synthesis of $O_2^{\bullet-}$. Even if

276 LOX is not known to be directly involved in $O_2^{\bullet-}$ production, it was suggested that extracellular

277   LOX may play an important role by competing with Prx for fatty acids and producing reactive

278   electrophiles that coordinate signaling responses [53].

279   The electrochemical method with the employment of different modified electrodes have

280   been successfully standardized and applied for detection of varied ROS including $O_2^{\bullet-}$ during

281   the recent past [69-71]. The polymeric iron-porphyrin-based modified carbon electrode is a

282   useful tool and provides a direct method for real-time monitoring and precise detection of $O_2^{\bullet-}$ in

283   biological samples *in-situ* [71]. The kinetic measurement showing the production of $O_2^{\bullet-}$ for a

284   long   range   of   time   (minutes)   presented   in   our   study

285   (https://ecs.confex.com/ecs/229/webprogram/Paper70675.html) have been demonstrated and thus

286   opens a new area of investigation which have always been difficult to explore using other

287   available methods such as EPR spin trapping spectroscopy, fluorescence microscopy and other

288   biochemical methods etc. Thus, the electrode has strong potential for wide application in plant

289   research for the specific and sensitive detection of $O_2^{\bullet-}$ and the kinetic behavior in real-time. In

290   addition to points mentioned above, using synthetic porphyrin has an additional advantage. To

291   date, $O_2^{\bullet-}$ sensors based on naturally derived enzyme (e.g. SOD, Cyt. c) have been developed

292   [72]. However, enzymes on the sensor are likely to be denatured. In contrast, the porphyrin based

293   sensor can be used without denaturation. At the same time, the current method is cost effective.

294   Certain limitations exist; the current polymeric iron-porphyrin-based modified carbon electrodes

295   are light-sensitive, which might hinder its photo-electrochemical applicability [73]. In the current

296   study, we present our polymeric iron-porphyrin based modified carbon electrode for application

297   in real-time monitoring and precise detection of $O_2^{\bullet-}$ in biological system. It is claimed to bear a

298   potential for its wide application in plant research for specific and sensitive detection of $O_2^{\bullet-}$.

299

300

301   **FIGURE LEGENDS**

302   **Figure 1** Reaction mechanism and experimental setup. (A) Schematic illustration of the reaction

303   mechanism for the amperometric detection of O2•− using the polymeric iron-porphyrin-based

304   modified carbon electrode depicting the reduction-oxidation cycle leading to generation of the

305   oxidation current. (B) Schematic illustration of the experimental setup for the electrochemical

306   measurements. The stimulation was performed using a glass capillary, and the polymeric iron-

307   porphyrin-based modified carbon electron was positioned at a distance of 1 mm using a motor-

308   driven XYZ microscopic stage. (C) The in vivo generation of O2 •− was measured using a

309   polymeric iron-porphyrin-based modified carbon electron (working electrode, WE), platinum

310   wire (counter electrode, CE) and Ag/AgCl (reference electrode, RE).

311   **Figure 2: Calibration curve.** Changes in oxidation current measured using iron-porphyrin-

312   based modified carbon electrode by exogenous addition of a standard known concentration of

313    $O_2^{\bullet-}$ generated *in situ* using X/XO system in the concentration range of 0.4 to 1.3μM.

314   **Figure 3: Real-time monitoring of the oxidation current of $O_2^{\bullet-}$ from spinach leaves.** The

315   kinetics of the production of $O_2^{\bullet-}$ were measured using a polymeric iron-porphyrin-based

316   modified carbon electrode on non-wounded spinach leaves.

317   **Figure 4: Real-time monitoring of oxidation current for $O_2^{\bullet-}$ during wounding** Kinetics of

318   the production of $O_2^{\bullet-}$ was measured using polymeric iron porphyrin based modified carbon

319   electrode during wounding in spinach leaves. The wounding in spinach leaves was done 1 time

320   (A) and multiple times (B) close to the site of electrode during the measurement and oxidation

321   current for $O_2^{\bullet-}$ was measured.

322 **Figure 5: Real-time monitoring of the oxidation current of $O_2^{\bullet-}$ during wounding.** The

323 kinetics of the production of $O_2^{\bullet-}$ were measured using a polymeric iron-porphyrin-based

324 modified carbon electrode during wounding in spinach leaves. The wounding of spinach leaves

325 was performed during the measurement, and the oxidation current for $O_2^{\bullet-}$ was measured for

326 approximately 30 min. The effect of SOD on the oxidation current was measured in the presence

327 of SOD (400 U ml^{-1}) added exogenously during the measurement.

328 **Figure 6: Real-time monitoring of oxidation current for $O_2^{\bullet-}$ during wounding.** Kinetics of

329 the production of $O_2^{\bullet-}$ was measured using polymeric iron porphyrin based modified carbon

330 electrode during wounding in spinach leaves. The wounding in spinach leaves was done during

331 the measurement and oxidation current for $O_2^{\bullet-}$ was measured for a duration of about 30 min.

332 Effect of SOD was measured in the presence of SOD (400U ml^{-1}) added exogenously during the

333 measurement at the point of maximum oxidation current.

334 **Table 1: Calculation.** Superoxide anion radical ($O_2^{\bullet-}$) concentration calculated using standard

335 calibration curve (R^2= 0.9918) (Fig. 2). The total change in oxidation current was found to be 1.5

336 nA (Δi) for minimal dose of injury (Fig. 4A) and 7.5 nA (Δi) for injury at multiple sites (Fig. 4B).

337 The total $O_2^{\bullet-}$ concentration was found to be equivalent to 40 nM (Fig. 4A) and 200 nM (Fig.

338 4B) at 60 sec and 300 sec, respectively.

339

340 **SUPPLEMENTARY DATA**

341 ***Supplementary data S1:*** Photographs of glass capillary (4 nos.) each with an inner diameter of

342 about 1.2mm and wall thickness of 200μm used for inducing mechanical injury in spinach leaves.

343   **II.** (A) Photograph of Spinach leaves in the experimental setup. For each measurement, young

344   spinach leaves of size approximately 8-10mm were chosen. (B) Photographs of petriplate with

345   Spinach leaves showing the arrangement of electrodes. **III.** Photographs of Spinach leaves

346   showing its state after mechanical injury with glass capillary. Injury was made 1 time (A), 5

347   times (B) and 20 times (C). **IV.** Kinetics of the production of $O_2^{\cdot-}$ measured using polymeric iron

348   porphyrin based modified carbon electrode during wounding in spinach leaves (arrow indicates

349   mechanical wounding). The wounding in spinach leaves was done 20 times close to the site of

350   electrode during the measurement and oxidation current for $O_2^{\cdot-}$ was measured.

351

352   ***Supplementary data S2:*** DPV for the electropolymerized [Fe(im)2(ttp)]Br complex recorded in

353   an aqueous electrolyte solution containing phosphate buffer (pH 7.2).

354

355   ***Supplementary data S3:*** EMPO-OOH adduct EPR spectra were measured in the presence of 25

356   mM EMPO, 40 mM phosphate buffer (pH 7.2) in the absence and presence of xanthine (1 mM)

357   and xanthine oxidase (0.2 U ml^{-1}). Panel (A) shows the spectra measured in the phosphate buffer

358   only (trace a) and X/XO system (trace b); (B) mean value ±SD, n=3, of the EMPO-OOH adduct

359   EPR spectra. The intensity of the EPR signal depicted in (B) was evaluated by measuring the

360   relative height of the central peak of the first derivative of the EPR absorption spectrum.

361

362   ***Supplementary data S4:*** Kinetics of the production of $O_2^{\cdot-}$ was measured using polymeric iron

363   porphyrin based modified carbon electrode in the chemical system (phosphate buffer) in the

364   presence of SOD (400U ml-1).

365

366 **REFERENCES**

367 1. Ledford HK, Chin BL, and Niyogi KK. Acclimation to singlet oxygen stress in

368 Chlamydomonas reinhardtii. Eukaryotic Cell. 2007; 6: 919–930.

369 2. Alessandro A, Osto LD, Aprile A, Carillo P, Roncaglia E, Cattivelli L, Bassi R. Reactive

370 oxygen species and transcript analysis upon excess light treatment in wild-

371 type *Arabidopsis thaliana* vs a photosensitive mutant lacking zeaxanthin and lutein. BMC

372 Plant Biology. 2011; 11: 62.

373 3. Foyer CH, and Shigeoka S. Understanding Oxidative Stress and Antioxidant Functions to

374 Enhance Photosynthesis. Plant Physiology. 2011; 155: 93–100.

375 4. Laloi C, and Havaux M. Key players of singlet oxygen-induced cell death in plants.

376 Frontiers in Plant Science. 2015; 6: 39.

377 5. Tripathy BC, Oelmüller R. Reactive oxygen species generation and signaling in plants.

378 Plant Signaling and Behavior. 2012; 7(12): 1621–1633.

379 6. Elstner EF. Mechanisms of oxygen activation in different compartments of plant cells,

380 in Active Oxygen/Oxidative Stress and Plant Metabolism, E. J. Pell and K. L. Steffen,

381 Eds., pp. 13–25, American Society of Plant Physiologists, Rockville, Md, USA. 1991.

382 7. Foyer CH, and Harbinson J. "Oxygen metabolism and the regulation of photosynthetic

383 electron transport," in Causes of Photooxidative Stresses and Amelioration of Defense

384 Systems in Plants, C. H. Foyer and P. Mullineaux, Eds., pp. 1–42, CRC Press, Boca

385 Raton, Fla, USA. 1994.

386 8. Asada K. Radical production and scavenging in the chloroplasts," in Photosynthesis and

387 the Environment, N. R. Baker, Ed., pp. 123–150, Kluwer, Dordrecht, The Netherlands.

388 1996.

389   9. Turrens JF. Mitochondrial formation of reactive oxygen species. Journal of Physiology.
390   2003; 552: 335–344.

391   10. Liu Y, Ren D, Pike S, Pallardy S, Gassmann W, and Zhang S. Chloroplast-generated
392   reactive oxygen species are involved in hypersensitive response-like cell death mediated
393   by a mitogen-activated protein kinase cascade. Plant Journal. 2007; 51: 941–954.

394   11. Murphy MP. How mitochondria produce reactive oxygen species. Biochemical Journal.
395   2009; 417: 1–13.

396   12. Miller G, Shulaev V, Mittler R. Reactive oxygen signaling and abiotic stress. Physiologia
397   Plantarum. 2008; 133(3): 481–489.

398   13. Gill SS, and Tuteja N. Reactive oxygen species and antioxidant machinery in abiotic
399   stress tolerance in crop plants. Plant Physiology and Biochemistry. 2010; 48: 909–930.

400   14. Foyer CH, Noctor G. Redox homeostasis and antioxidant signaling: a metabolic interface
401   between stress perception and physiological responses. Plant Cell. 2005; 17: 1866–1875.

402   15. Asada K. Production and scavenging of reactive oxygen species in chloroplasts and their
403   functions. Plant Physiology. 2006; 141: 391–396.

404   16. Miller G, Schlauch K, Tam R, Cortes D, Torres MA, Shulaev V, Dangl JL, Mittler R.
405   The plant NADPH oxidase RBOHD mediates rapid systemic signaling in response to
406   diverse stimuli. Science Signaling. 2009; 2(84): 45–49.

407   17. Bhattacharjee S. Sites of generation and physicochemical basis of formation of reactive
408   oxygen species in plant cell, in Reactive Oxygen Species and Antioxidants in Higher
409   Plants. S. Dutta Gupta, Ed., pp. 1–30, CRC Press, New York, NY, USA. 2010.

410   18. Choudhury S, Panda P, Sahoo L, and Panda SK. Reactive oxygen species signalling in
411   plants under abiotic stress. Plant Signaling & Behaviour. 2013; 8: e23681.

412 19. McDowell RE, Amsler MO, Li Q, Lancaster Jr JR, Amsler CD. The immediate wound-

413   induced oxidative burst of Saccharina latissimi depends on light via photosynthetic

414   electron transport. Journal of Phycology. 2015; 51: 431–441.

415 20. Legendre L, Rueter S, Heinstein PF, Low PS. Characterization of the oligogalacturonide-

416   induced oxidative cells. Plant Physiology. 1993; 102: 233–240.

417 21. John M, Rohrig G, Schmidt J, Walden R, Schell J. Cell signaling by oligosaccharides.

418   Trends in Plant Science. 1997; 2: 111–115.

419 22. Stennis M, Chandra S, Ryan C, Low P. Systemin potentiates the oxidative burst in

420   cultured tomato cells. Plant Physiology. 1998; 117: 1031–1036.

421 23. Murphy TM, Asard H, Cross AR. Possible sources of reactive oxygen during the

422   oxidative burst in plants. In: Asard, H., Berczi, A. (Eds.), Plasma Membrane Redox

423   Systems and their Role in Biological Stresses and Disease. Kluwer Academic Publishers,

424   Dordrecht, pp. 215–246. 1998.

425 24. Garces H, Durzan D, Pedroso MC. Mechanical stress elicits nitric oxide formation and

426   DNA fragmentation in *Arabidopsis thaliana*. Annals of Botany. 2001; 87: 567–574.

427 25. Jih PJ, Chen YC, Jeng ST. Involvement of hydrogen peroxide and nitric oxide in

428   expression of the ipomoelin gene from sweet potato. Plant Physiology. 2003; 132: 381–

429   389.

430 26. Morker KH, Roberts MR. Light as both an input and an output of wound-induced

431   reactive oxygen formation in Arabidopsis leaves. Plant Signaling and Behaviour. 2011;

432   6(8): 1-3.

27. Vylegzhaninat NN, Gordon LK, Minibayeva FV, Kolesnikov OP. Superoxide Production as a Stress Response of Wounded Root Cells: ESR Spin-Trap and Acceptor Methods. Applied Magnetic Resonance. 2001; 21: 63-70.

28. Misra HR, Fridovich I. The Univalent Reduction of Oxygen by Reduced Flavins and Quinones. The Journal of Biological Chemistry. 1972; 247: 188-192.

29. Barber MJ, Kay CJ. Superoxide production during reduction of molecular oxygen by assimilatory nitrate reductase. Archives of Biochemistry and Biophysics. 1996; 326: 227-232.

30. Wohlgemuth H, Mittelstrass K, Kschieschan S, Bender J, Weigel HJ, Overmyer K, Kangasjärvi J, Sandermann H, Langebartels C. Activation of an oxidative burst is a general feature of sensitive plants exposed to the air pollutant ozone. Plant Cell Environment. 2002; 25: 717–726.

31. Von GM, Schlosser E, Neubacher H. Evidence from electron-spin resonance for the formation of free radicals during infection of Avena sativa by Drechslera spp. Physiology and Molecular Plant Pathology. 1993; 42: 405–412.

32. Anderson AA, Rogers K, Tepper CS, Blee K, Cardon J. Timing of molecular events following elicitor treatment of plant cells. Physiology and Molecular Plant Pathology 1991; 38: 1–13.

33. Doke N. Involvement of superoxide anion generation in the hypersensitive response of potato tuber tissues to infection with an incompatible race of Phytophthora infestans and to the hyphal wall components. Physiological Plant Pathology. 1983; 23: 345–357.

34. Doke N. Generation of superoxide anion by potato tuber protoplasts during the hypersensitive response to hyphal wall components of Phytophthora infestans and

456   specific inhibition of the reaction by suppressors of hypersensitivity. Physiological Plant

457   Pathology. 1983; 23: 359–367.

458   35. Doke N. NADPH-dependent $O_2^{\bullet -}$ generation in membrane fractions isolated from

459   wounded potato tubers inoculated with Phytophthora infestans. Physiological Plant

460   Pathology. 1985; 27: 311–322.

461   36. Prasad A and Pospíšil P. Ultraweak photon emission induced by visible light and

462   ultraviolet A radiation via photoactivated skin chromophores: in vivo charge coupled

463   device imaging. Journal of Biomedical Optics. 2012; 17(8): 85004.

464   37. Prasad A and Pospíšil P. Towards the two-dimensional imaging of spontaneous ultra-

465   weak photon emission from microbial, plant and animal cells. Scientific Reports. 2013; 3:

466   1211.

467   38. Pospíšil P, Prasad A and Rác M. Role of reactive oxygen species in ultra-weak photon

468   emission in biological systems. Journal of Photochemistry and Photobiology B: Biology

469   .2014; 139: 11-23.

470   39. Halliwell B, Gutteridge JMC. Free Radicals in Biology and Medicine, Ed 2. Clarendon

471   Press, Oxford, UK. 1989.

472   40. Bedioui F, Devynck J and Charreton CB. Immobilization of metalloporphyrins in

473   electropolymerized films: design and applications. Accounts of Chemical Research.

474   1995; 28 (1), 30-36

475   41. Deronzier A, and Moutet JC. Polypyrrole films containing metal complexes: syntheses

476   and applications. Coordination Chemistry Reviews. 1996; 147, 339-371.

477   42. Yim HS, Kibbey CE, Ma SC, Kliza DM, Liu D, Park SB, Terre CE and Meyerhoff ME.

478   Polymer membrane-based ion-, gas- and bio-selective potentiometric sensors. Biosensors

479   and Bioelectronics. 1993; 8,1-38.

480   43. Bedioui F, Trevin S, and Devynck J. Chemically modified microelectrodes designed for

481   the electrochemical determination of nitric oxide in biological systems. Electroanalysis.

482   1996; 8, 1085-1091.

483   44. Matsuoka R, Igarashi M, Kondo T, Aikawa T, and Yuasa M. Biomimetic

484   antithrombogenic electrochemical superoxide anion radical sensor. Journal of the

485   Electrochemical Society. 2014; 161:6.

486   45. Olson JS, Ballou DP, Palmer GS, Massey V. The Reaction of Xanthine Oxidase with

487   Molecular Oxygen. The Journal of Biological Chemistry. 1974; 249: 4350-4362.

488   46. Richter C. Redox intermediates between O_2 and H_2O. Membrane Biochemistry. A

489   Laboratory Manual on Transport and Bioenergetics. doi: 10.1007/978-3-642-67530-0_12.

490   1979.

491   47. Porras AG, Olson JS, Palmer G. The reaction of reduced xanthine oxidase with oxygen.

492   Kinetics of peroxide and superoxide formation. The Journal of Biological Chemistry.

493   1981; 256: 9096-9103.

494   48. Zuo L, Nogueira L and Hogan MC. Reactive oxygen species formation during tetanic

495   contractions in single isolated Xenopus myofibers. Journal of Applied Physiology. 2011;

496   111: 898-904.

497   49. Zuo L, Shiah A, Roberts WJ, Chien MT, Wagner PD and Hogan MC. Low P_{O2}

498   Conditions Induce Reactive Oxygen Species Formation during Contractions in Single

499   Skeletal Muscle Fibers. American Journal of Physiology. Regulatory, integrative and

500   Comparative Physiology. 2013; 304 (11): R1009-16.

501   50. Zuo L, Hallman AH, Roberts WJ, Wagner PD, Hogan MC. Superoxide release from

502   contracting skeletal muscle in pulmonary TNF-α overexpression mice. American Journal

503   of Physiology. Regulatory, integrative and Comparative Physiology. 2014; 306(1): R75-

504   R81.

505   51. Zuo L, Christofi FL, Wright VP, Bao S, Clanton TL. Lipoxygenase-dependent

506   superoxide release in skeletal muscle. Journal of Applied Physiology. 2004; 97(2):661-

507   668.

508   52. Murphy TM, Auh CK. The Superoxide Synthases of Plasma Membrane Preparations

509   from Cultured Rose Cells. Plant Physiology. 1996; 110: 621-629.

510   53. Doke N, Miura J, Sanchez LM, Park HJ, Noritake T, Yoshioka H, Kawakita K. The

511   oxidative burst protects plants against pathogen attack: mechanism and role as an

512   emergency signal for plant bio-defence- a review. Gene. 1996; 179: 45-5.

513   54. Watanabe T, Sakai S. Effects of active oxygen species and methyl jasmonate on

514   expression of the gene for a wound-inducible 1-aminocyclopropane-1-carboxylate

515   synthase in winter squash (C. maxima). Planta. 1998; 206: 570-576.

516   55. Flor-Henry M, McCabe TC, Bruxelles GL de, Roberts MR. Use of a highly sensitive

517   two-dimensional luminescence imaging system to monitor endogenous bioluminescence

518   in plant leaves. BMC Plant Biology. 2004; 4: 19.

519   56. Roach T, Colville L, Beckett RP, Minibayeva FV, Havaux M, Kranner I. A proposed

520   interplay between peroxidase, amine oxidase and lipoxygenase in the wounding-induced

521   oxidative burst in Pisum sativum seedlings. Phytochemistry. 2015; 112: 130–138.

522   57. Minibayeva F, Kolesnikov O, Chasov A, Beckett RP, Luthje S, Vylegzhanina N, Buck F

523   and Bottger M. Wound-induced apoplastic peroxidases activities: their roles in the

524   production and detoxification of reactive oxygen species. Plant Cell Environment. 2009;

525   32: 497–508.

526   58. Roach T, Beckett RP, Minibayeva FV, Colville L, Whitaker C, Chen H, Bailly C,

527   Kranner I. Extracellular superoxide production, viability and redox poise in response to

528   desiccation in recalcitrant Castanea sativa seeds. Plant Cell Environment. 2009; 33: 59–

529   75.

530   59. Whitaker C, Beckett RP, Minibayeva FV, Kranner I. Production of reactive oxygen

531   species in excised, desiccated and cryopreserved explants of Trichiliadregeana. South

532   African Journal of Botany. 2010; 76: 112–118.

533   60. Li JLY, Sulaiman M, Beckett RP, Minibayeva FV. Cell wall peroxidases in the liverwort

534   Dumortiera hirsuta are responsible for extracellular superoxide production, and can

535   display tyrosinase activity. Physiologia Plantarum. 2010; 138: 474–484.

536   61. Liers C, Ullrich C, Hofrichter M, Minibayeva FV, Beckett RP. Oxidoreductases from

537   lichenized ascomycetes: purification and characterization of a heme-peroxidase from

538   Leptogium saturninum that oxidizes high-redox potential substrates. Fungal Genetics and

539   Biology 2011; 48: 1139–1145.

540   62. Rea G, Metoui O, Infantino A, Federico R, Angelini R. Copper amine oxidase expression

541   in defense responses to wounding and Ascochyta rabiei invasion. Plant Physiology. 2002;

542   128: 865–875.

543   63. Cona A, Rea G, Botta M, Corelli F, Federico R, Angelini R. Flavin containing polyamine

544   oxidase is a hydrogen peroxide source in the oxidative response to the protein

545   phosphatase inhibitor cantharidin in Zea mays L. Journal of Experimental Botany. 2006;

546   57: 2277–2289.

547 64. Yoda H, Hiroi Y, Sano H. Polyamine oxidase is one of the key elements for oxidative

548   burst to induce programmed cell death in tobacco cultured cells. Plant Physiology. 2006;

549   142: 193–206.

550 65. Angelini R, Tisi A, Rea G, Chen MM, Botta M, Federico R, Cona A. Involvement of

551   polyamine oxidase in wound healing. Plant Physiology. 2008; 146: 162–177.

552 66. Roy P, Roy SK, Mitra A, Kulkarni AP. Superoxide generation by lipoxygenase in the

553   presence of NADH and NADPH. Biochimica et Biophysica Acta. 1994; 1214: 171–179.

554 67. Upchurch RG. Fatty acid unsaturation, mobilization, and regulation in the response of

555   plants to stress. Biotechnology Letters. 2008; 30: 967–977.

556 68. Higdon A, Diers AR, Oh, J, Landar Y, Darley-Usmar VM. Cell signalling by reactive

557   lipid species: new concepts and molecular mechanisms. Biochemical Journal. 2012; 442:

558   453–464.

559 69. Groenendaal Jonas F, Freitag D, Pielartzik H, and Reynolds JR. Poly(3,4

560   ethylenedioxythiophene) and Its Derivatives: Past, Present, and Future. Advanced

561   Materials. 2000; 12: 481.

562 70. Yuasa, M and Oyaizu, K. Electrochemical Detection and Sensing of Reactive Oxygen

563   Species. Current Organic Chemistry. 2005; 9: 1685.

564 71. Yuasa M, Oyaizu K, Yamaguchi A, Ishikawa M, Eguchi K, Kobayashi T, Toyoda Y, and

565   Tsutsui S. Electrochemical sensor for superoxide anion radical using polymeric iron

566   porphyrin complexes containing axial 1-methylimidazole ligand as cytochrome c mimics.

567   Polymers for Advanced Technologies. 2005; 16: 287-292.

568   72. Di J, Bi S, Zhang M. Third-generation superoxide anion sensor based on superoxide

569   dismutase directly immobilized by sol–gel thin film on gold electrode. Biosensors and

570   Bioelectronics. 2004; 19: 1479–1486.

571   73. Brett CMA and Brett AMCFO. Surface modified electrode-reasons and advantages”

572   in Surface Engineering: Surface modification of materials, R. Kossowsky and S.C.

573   Singhal, Ed., pp. 656–664, Westinghouse R &D center, Pittsburg, USA. 1984.

574   74. Prasad A, Kikuchi H, Inoue KY, Suzuki M, Sugiura Y, Sugai T, Tomonori A, Tada M,

575   Kobayashi M, Matsue T and Kasai S. Simultaneous Real-Time Monitoring of Oxygen

576   Consumption and Hydrogen Peroxide Production in Cells Using Our Newly Developed

577   Chip-Type Biosensor Device. Frontiers in Physiology. 2016; 7: 109.

Calculation

Superoxide anion radical ($O_2{}^{\bullet-}$) concentration calculated using standard calibration curve (R^2= 0.9918) (Fig. 2). The total change in oxidation current was found to be 1.51 nA (Δi) for minimal dose of injury (Fig. 4A) and 7.47 nA (Δi) for injury at multiple sites (Fig. 4B). The total $O_2{}^{\bullet-}$ concentration was found to be equivalent to 40 nM (Fig. 4A) and 198 nM (Fig. 4B) at 60 sec and 300 sec, respectively.

	A	B
Δi (nA)	1.51	7.47
Δt (sec)	60	300
$O_2^{\bullet-}$ (nM)	**40**	**198**

Figure_1.pdf
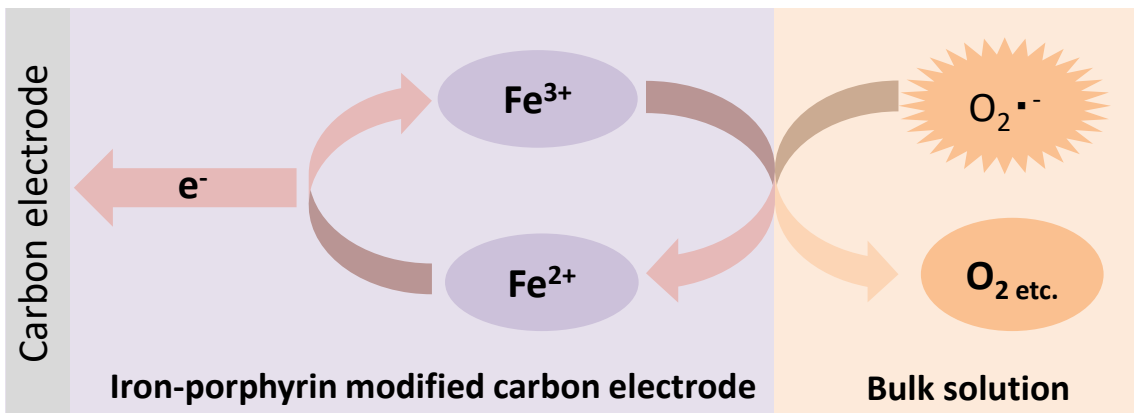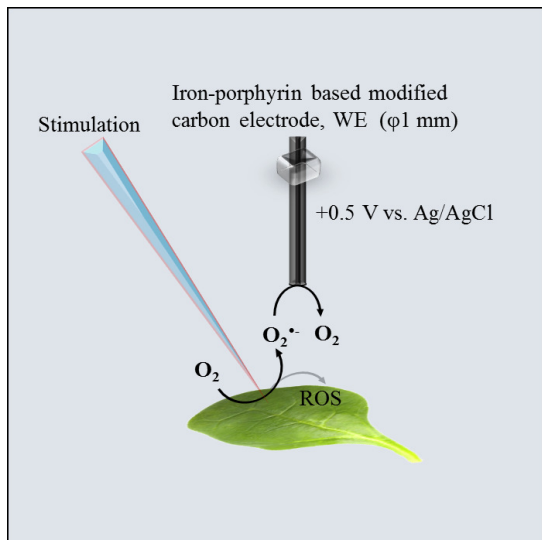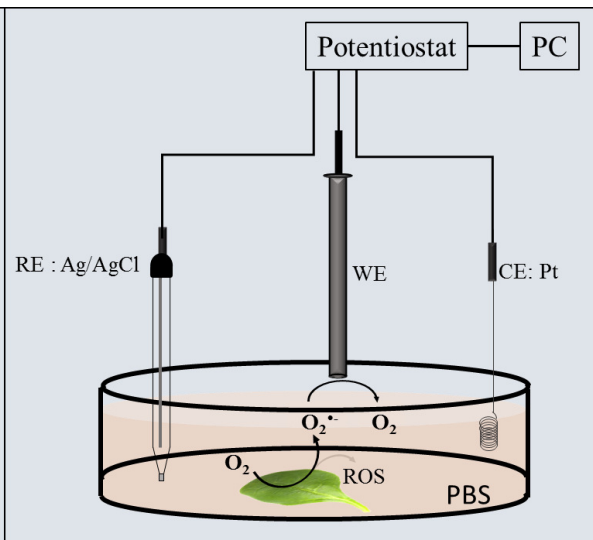
Calibration curve

Changes in oxidation current measured using iron-porphyrin-based modified carbon electrode by exogenous addition of a standard known concentration of $O_2^{\cdot-}$ generated *in situ* using XAN/XOD system in the concentration range of 0.4 to 1.3µM.
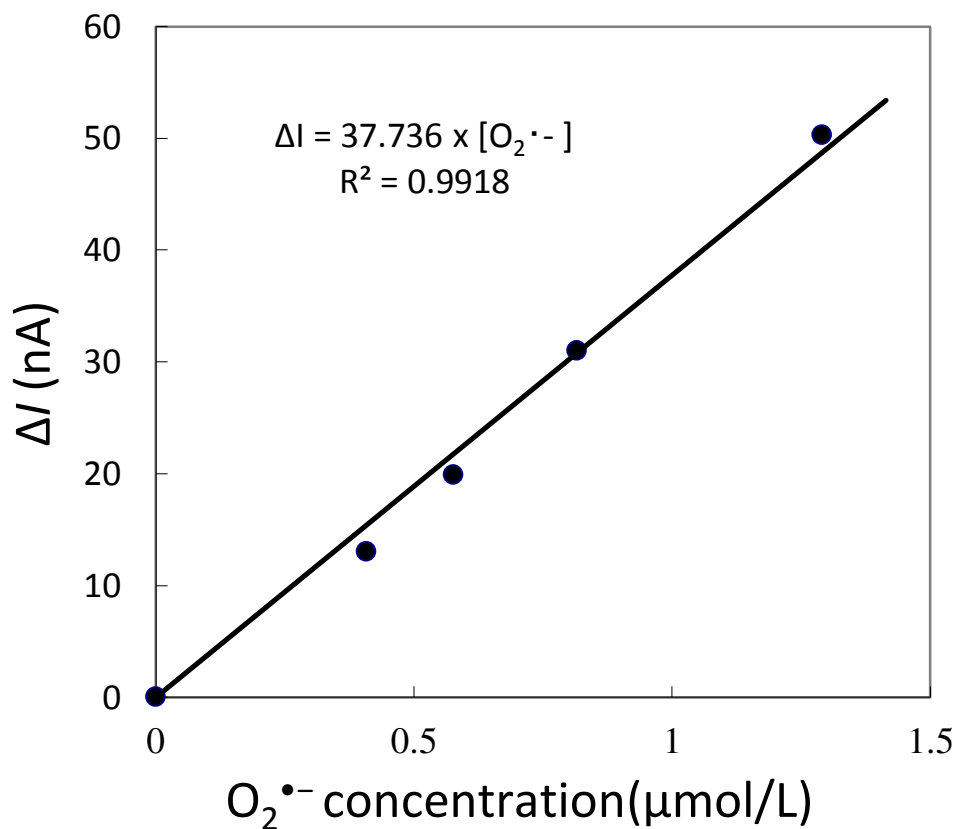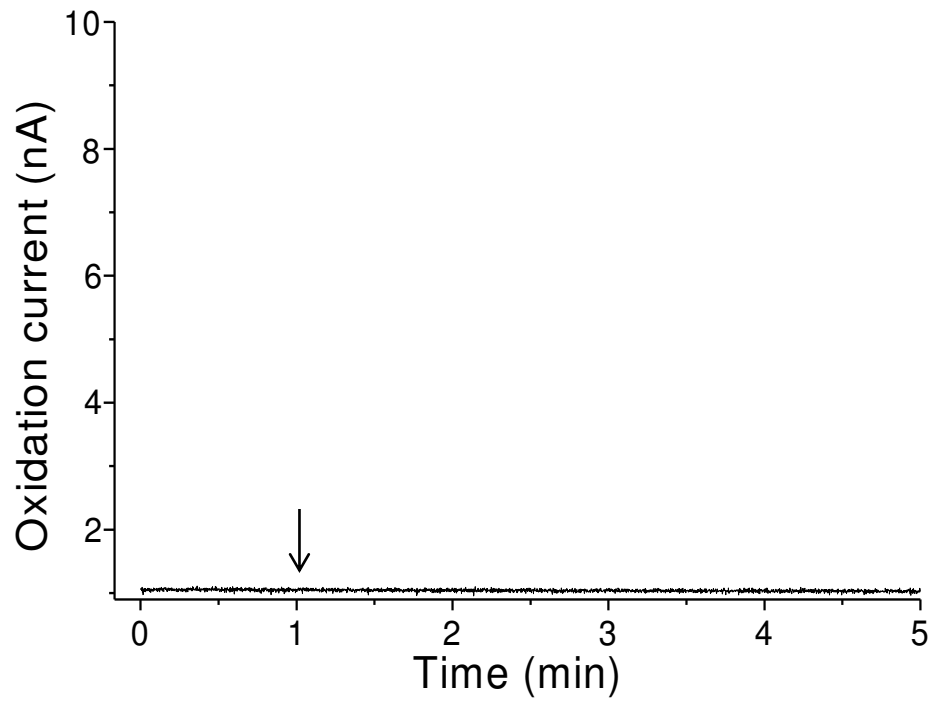
Figure_3.pdf

Real-time monitoring of oxidation current for $O_2{}^{\bullet-}$ during wounding

Kinetics of the production of $O_2{}^{\bullet-}$ was measured using polymeric iron porphyrin based modified carbon electrode during wounding in spinach leaves. The wounding in spinach leaves was done 1 time (A) and multiple times (B) close to the site of electrode during the measurement and oxidation current for $O_2{}^{\bullet-}$ was measured.
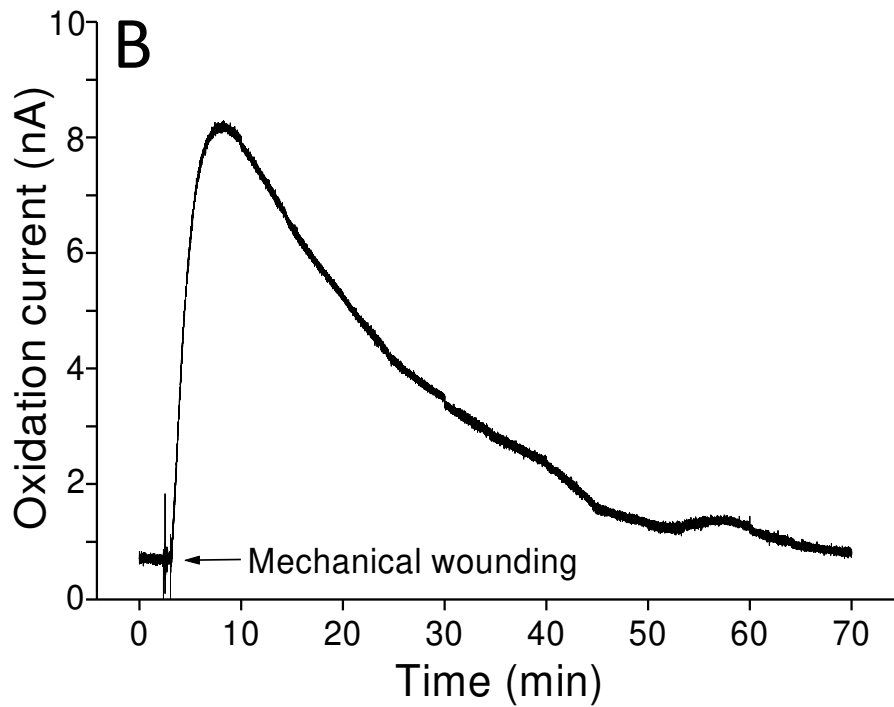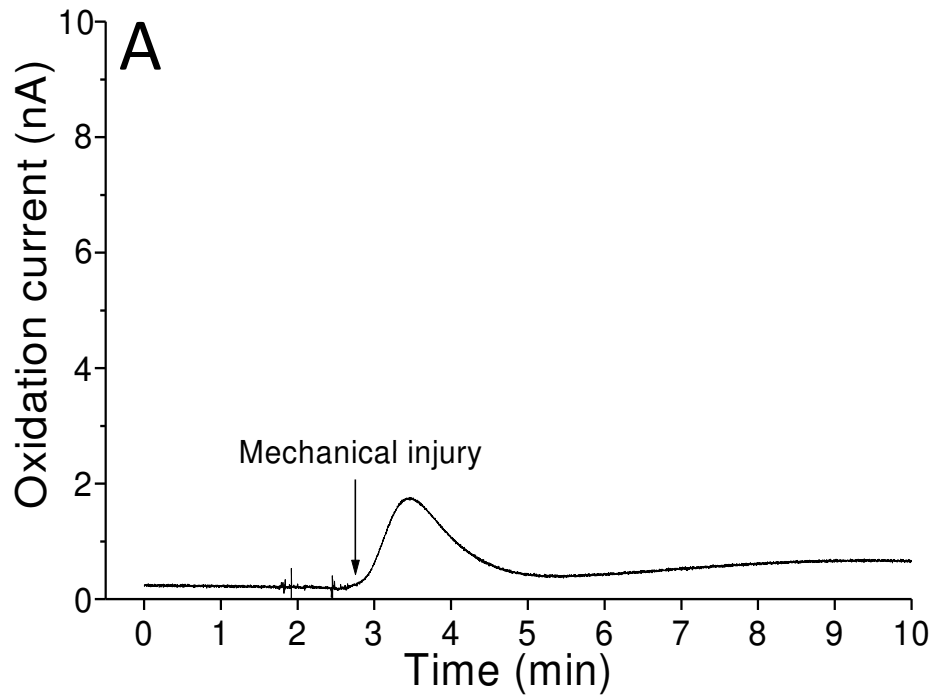
Real-time monitoring of the oxidation current of $O_2{}^{\bullet-}$ during wounding

The kinetics of the production of $O_2{}^{\bullet-}$ were measured using a polymeric iron-porphyrin-based modified carbon electrode during wounding in spinach leaves. The wounding of spinach leaves was performed during the measurement, and the oxidation current for $O_2{}^{\bullet-}$ was measured for approximately 30 min. The effect of SOD on the oxidation current was measured in the presence of SOD (400 U ml^{-1}) added exogenously during the measurement.

Figure_6.pdf